

# Arteriosclerosis, Thrombosis, and Vascular Biology



JOURNAL OF THE AMERICAN HEART ASSOCIATION

## MRI and Characterization of Atherosclerotic Plaque: Emerging Applications and Molecular Imaging

Robin P. Choudhury, Valentin Fuster, Juan J. Badimon, Edward A. Fisher and Zahi A. Fayad

*Arterioscler Thromb Vasc Biol.* 2002;22:1065-1074; originally published online April 25, 2002;  
doi: 10.1161/01.ATV.0000019735.54479.2F

*Arteriosclerosis, Thrombosis, and Vascular Biology* is published by the American Heart Association, 7272  
Greenville Avenue, Dallas, TX 75231

Copyright © 2002 American Heart Association, Inc. All rights reserved.  
Print ISSN: 1079-5642. Online ISSN: 1524-4636

The online version of this article, along with updated information and services, is located on the  
World Wide Web at:

<http://atvb.ahajournals.org/content/22/7/1065>

**Permissions:** Requests for permissions to reproduce figures, tables, or portions of articles originally published in *Arteriosclerosis, Thrombosis, and Vascular Biology* can be obtained via RightsLink, a service of the Copyright Clearance Center, not the Editorial Office. Once the online version of the published article for which permission is being requested is located, click Request Permissions in the middle column of the Web page under Services. Further information about this process is available in the [Permissions and Rights Question and Answer](#) document.

**Reprints:** Information about reprints can be found online at:  
<http://www.lww.com/reprints>

**Subscriptions:** Information about subscribing to *Arteriosclerosis, Thrombosis, and Vascular Biology* is online at:  
<http://atvb.ahajournals.org/subscriptions/>

## MRI and Characterization of Atherosclerotic Plaque Emerging Applications and Molecular Imaging

Robin P. Choudhury, Valentin Fuster, Juan J. Badimon, Edward A. Fisher, Zahi A. Fayad

**Abstract**—Noninvasive high-resolution magnetic resonance has the potential to image atherosclerotic plaque and to determine its composition and microanatomy. This review summarizes the rationale for plaque imaging and describes the characteristics of plaque by use of existing MRI techniques. The use of MRI in human disease and in animal models, particularly in rabbits and mice, is presented. Present and future applications of MRI, including real-time vascular intervention, new contrast agents, and molecular imaging, are also discussed. (*Arterioscler Thromb Vasc Biol.* 2002;22:1065-1074.)

**Key Words:** MRI ■ atherosclerosis ■ plaque ■ molecular imaging ■ mice

The introduction of percutaneous arteriography by Fariñas<sup>1</sup> in 1941 and selective coronary arteriography by Sones<sup>2</sup> in 1957 made clinical imaging of atherosclerosis possible. Arteriography provides useful anatomic information that has been used to guide decisions about treatment and to enable the delivery of therapy in the case of percutaneous interventions.<sup>3-5</sup> However, arteriography images only the vessel lumen and the silhouette of lesions that impinge on the lumen. Atherosclerosis can develop in the arterial wall and be accommodated by outward (or positive) arterial remodeling.<sup>6,7</sup> At sites of positive remodeling, lumen caliber may be unaltered or minimally altered and, therefore, not detected by arteriography. The importance of this has been highlighted in angiographic studies demonstrating that nonsevere stenoses are more often associated with acute coronary events than are severe coronary stenoses.<sup>8,9</sup> From a pathological perspective, plaques with large lipid cores and thin fibrous caps are more prone to rupture, leading to thrombosis and vascular events, than are plaques with small securely contained lipid cores and thick caps.<sup>10,11</sup> The present challenge is to develop imaging technology capable of characterizing atherosclerosis, particularly in human coronary arteries. This may allow identification (and treatment) of plaques that are at risk of future rupture and thrombosis.<sup>12</sup>

### See page 1064

Numerous imaging modalities, including thermography, near infra-red spectroscopy, Raman spectroscopy, ultrafast CT, and ultrasound have been applied to the characterization of plaque and are reviewed in detail elsewhere.<sup>13-15</sup> However, MRI has the greatest potential for clinical application. Magnetic resonance (MR) is well suited to this role because it is noninvasive, does not involve ionizing radiation, can be repeated serially, and provides high-resolution images of the vessel wall and lumen.

Atherosclerosis usually develops silently over many years, although significant lesions are commonly present as early as the second decade.<sup>16</sup> Lipid-lowering drugs have demonstrated efficacy and safety in the primary prevention of the complications of atherosclerosis,<sup>17,18</sup> but the present guidelines do not include the presence of subclinical atherosclerosis in decisions about therapy.<sup>19</sup> In the future, risk stratification, which includes noninvasive identification and characterization of atherosclerosis, may direct the type and intensity of treatment in individual patients, even before clinical disease has been allowed to manifest itself.

Our expanding knowledge of plaque composition, biology, and behavior demands that imaging modalities provide quantitative and qualitative information about the plaque.<sup>10,20-23</sup> The present review will summarize the rationale for plaque

Received February 22, 2002; revision accepted April 11, 2002.

From the Department of Cardiovascular Medicine (R.P.C.), University of Oxford, John Radcliffe Hospital, Oxford, UK, and The Zena and Michael A. Wiener Cardiovascular Institute (V.F., J.J.B., E.A.F., Z.A.F.), Mount Sinai School of Medicine, New York, NY.

Correspondence to Zahi Fayad, PhD, The Cardiovascular Institute, Mount Sinai School of Medicine, Box 1030, 1 Gustave L. Levy Place, New York, NY 10029-6574. E-mail zahi.fayad@mssm.edu

© 2002 American Heart Association, Inc.

*Arterioscler Thromb Vasc Biol.* is available at <http://www.atvbaha.org>

DOI: 10.1161/01.ATV.0000019735.54479.2F

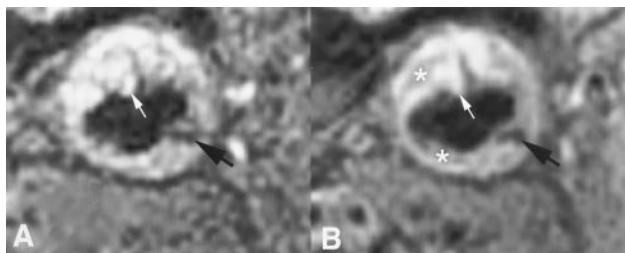


**Figure 1.** A 67-year-old male with atherosclerotic disease in the common carotid artery imaged with in vivo high-resolution MR. Multicontrast (T1W, PDW [not shown], and T2W) MR images are obtained to characterize all the plaque components. A, T1W image. B, T2W image. A complex lesion is detected with a fissure (at 12 o'clock). Black arrows indicate calcium; asterisk, lipid deposits; and white arrows, thrombus.

imaging, provide a technical overview of MRI, and describe the characteristics of plaque by use of existing MRI techniques. Present and future applications of MRI, including targeted contrast and molecular imaging, will also be discussed.

### Principles of MRI

MRI has emerged as the potential leading noninvasive in vivo modality for atherosclerotic plaque imaging in experimental animals<sup>24–30</sup> and in humans.<sup>26,31–35</sup> The principles of MRI are described in detail elsewhere.<sup>36–38</sup> In brief, MR characterizes plaque on the basis of the biophysical and biochemical properties of its different components. Representative MR images can be seen in Figures 1 through 4.

During the examination, the subject is positioned in a high-external-static magnetic field (usually 1.5 T for human studies; see Tables 1 and 2), which aligns the protons in the body. Thus far, the application of an external static magnetic field to the spins will result in a net magnetization that is parallel to the applied field. This longitudinal magnetization is not detected. Instead, the longitudinal magnetization must be converted into a transverse magnetization, perpendicular to the applied static field, before it can be detected. This conversion can be accomplished by the application of a time-varying electromagnetic radiofrequency (RF) pulse, applied at the resonance frequency. The protons can then absorb that energy. The transverse magnetization created does not remain in the transverse plane indefinitely. After the RF pulse is turned off, 3 events begin to happen simultaneously: (1) The absorbed RF energy is retransmitted (at the resonance frequency). This is the “MRI signal.” (2) The excited spins begin to return to the original equilibrium longitudinal magnetization. The rate at which the recovery occurs is deter-

mined by the spin-lattice relaxation time (T1). Fortunately, the T1 relaxation times vary among tissue types, providing a highly useful means of generating image contrast. (3) Initially, in phase, the excited protons begin to dephase at a rate characterized by the spin-spin relaxation time (T2). The T2 relaxation times also vary with tissue type, providing another means of generating tissue contrast. The resulting “MRI signal” is detected by receiving RF coils.

Images in which most of the contrast between tissues is derived from differences in tissue T1 are termed T1-weighted (T1W) and, analogously, T2-weighted (T2W) images. A proton density-weighted (PDW) image is obtained when the differences in contrast are proportional to the density of water and fat protons within the tissue.

Three additional mutually perpendicular magnetic fields (gradient fields) are applied during MRI: 1 to select the slice and 2 to encode spatial information. As a result, each voxel within the imaged tissue is uniquely identified.

### Determination of Plaque Components With MR

Atherosclerotic plaques are of heterogeneous composition. Angiographic and pathological<sup>21,23</sup> studies have determined the plaque types at greatest risk of acute rupture or erosion. In human coronary arteries, location,<sup>39</sup> geometry,<sup>10,40</sup> and composition<sup>10,40–43</sup> are all useful indicators of vulnerability. In particular, the presence of a large extracellular lipid core, thin fibrous cap, and inflammatory cell infiltrate indicates plaques at risk.<sup>10,44</sup> Can MRI rise to the challenge of discerning these factors?

### Plaque Characterization by Non-Contrast-Enhanced MRI

In MRI, the emitted RF signal differs between the nuclei of different atoms and further varies according to the molecular environment of the nuclei. In this way, it is possible to obtain quantitative information about specific molecules of interest within a given tissue. In early MR studies of atherosclerosis, characterization was directed toward chemical shift imaging by use of the lipid signal.<sup>45,46</sup> These studies were designed to image plaque lipids with long T2 and short T1 relaxation times, similar to triglycerides. However, unlike periaortic fat, which is composed of fatty acyl triglycerides, the lipid components of the plaque are predominantly cholesterol, cholesteryl ester, and phospholipid,<sup>47</sup> whose MR characteristics are different from the fat of adipose tissue.<sup>48</sup> Furthermore, chemical shift imaging aimed at directly imaging lipid components of the plaque is intrinsically disadvantaged, because

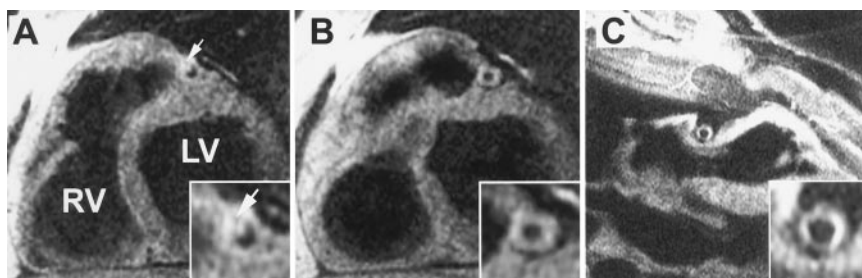


**Figure 2.** In vivo MR black-blood cross-sectional images of human coronary arteries demonstrating a plaque presumably with deposition of fat (arrow, panel A), a concentric fibrotic lesion (panel B) in the left anterior descending artery, and an ectatic, but atherosclerotic, right coronary artery (panel C). RV indicates right ventricle; LV, left ventricle. Figure modified from Fayad et al.<sup>34</sup>

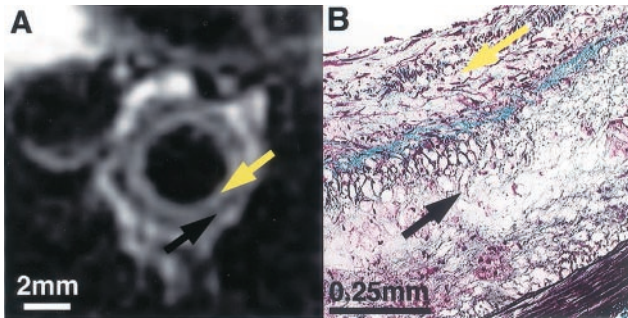


**Figure 3.** A, In vivo MR images (T2W) of rabbit abdominal aorta. B, Corresponding histopathological section (combined Masson elastin stain). MRI differentiates fibrotic (high-signal, yellow arrow) and lipid (low-signal, black arrow) components of the plaque. Figure modified from Helft et al.<sup>30</sup>

even in relative lipid-rich plaque, the signal from water predominates by  $\approx 10$ -fold.<sup>49,50</sup> For these reasons, recent studies have focused on MRI of water protons.<sup>50,51</sup>

By use of a combination of inherent MRI contrast generated in T1W, T2W, and PDW images (Table 1), it has been possible to determine plaque anatomy and composition in experimental animals,<sup>24,30</sup> in ex vivo specimens,<sup>33,50,52</sup> and in human carotid arteries (Figure 1)<sup>33,53</sup> and aortas in vivo.<sup>54</sup> Recently, atherosclerosis has also been identified, in vivo, in human coronary arteries.<sup>34,55,56</sup> These applications are discussed further below.

Toussaint et al<sup>33</sup> demonstrated that fibrous cap, lipid core, media, and adventitia could be distinguished by use of high-field/high-resolution MRI. Differences in water T2 contrast, ex vivo<sup>33,50</sup> and in vivo,<sup>33</sup> identified lipid core versus fibrous cap, normal media versus lipid core, and media versus adventitia. Compared with the fibrous cap or media, the atheromatous core is associated with a shortened water T2 and, therefore, appears dark compared with the adjacent cap and media, which appear bright on T2W images. Calcified

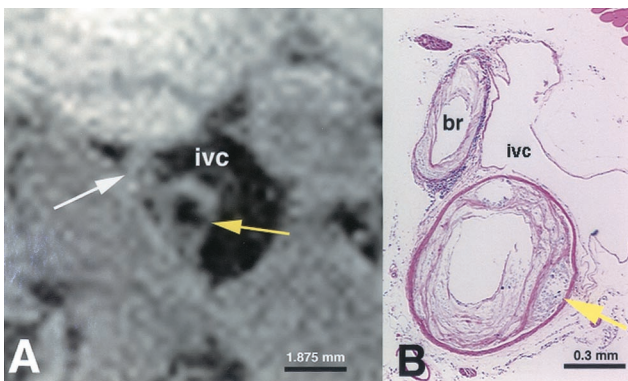


**Figure 4.** T1W MR image (magnified; see scale) of atherosclerotic lipid-rich complex plaque in an apoE-knockout (apoE-KO) mouse. MR pixel size is  $97 \times 97 \times 500 \mu\text{m}^3$ . At the top left of the abdominal aorta, an atherosclerotic small branch vessel (br) is seen by MR (panel A, white arrow) and by histopathology (panel B) in 21-month-old apoE-KO mouse. This lesion had a focal calcium deposit in abdominal aorta (yellow arrow) that appeared as a signal void (panel A) and was correlated with histopathological findings (panel B), as show by hematoxylin-eosin stain (original magnification  $\times 40$ ). Inferior vena cava (IVC) is shown at right of the abdominal aorta (A). Figure was modified from Fayad et al.<sup>27</sup>

areas of plaque do not generate appreciable signal because of the low water content, but they can be detected as areas of low signal (black) on T1W images.<sup>14,57</sup>

Characterization of plaque in vivo in humans has been achieved in the aorta and carotid artery.<sup>33,53</sup> Fayad et al<sup>54</sup> found good correlation of multicontrast MRI with aortic plaque quantification and characterization by using transesophageal echocardiography. Hatsukami et al<sup>53</sup> used a 3D multiple-overlapping thin-slab MR/multiple-overlapping thin-slice angiography/time-of-flight technique to image the fibrous cap of carotid arteries before endarterectomy. In their study of 22 patients undergoing carotid endarterectomy (with a best voxel size of  $254 \times 254 \times 1000 \mu\text{m}^3$ ), thick fibrous caps were seen as a dark band between the lumen (white) and the vessel wall (gray). The presence of a thin cap was inferred from the absence of any discernible dark band. Plaque rupture was identified in vivo by MRI in 8 of the 9 cases in which it was subsequently identified on the atherectomy specimens. Also, in human carotid arteries that were imaged in vivo, Yuan et al<sup>58</sup> have identified lipid core with sensitivity 85% and specificity 92% by using time-of-flight-based bright blood and spin-echo-based black blood multicontrast techniques. Although lipid-rich necrotic cores were typically hypointense with T2W, this was variable, and as reported previously,<sup>52</sup> the comparison of vessel wall appearances under different contrast weightings provided the greatest diagnostic yield.

The same authors have recently demonstrated the clinical significance of carotid plaque characterization.<sup>59</sup> In a case-control study of patients undergoing carotid endarterectomy, a recent (within 90-day) history of transient ischemic attack or stroke was strongly associated with the presence of thin or ruptured plaque identified preoperatively by MRI. The risk of recent ischemic neurological symptoms was increased by an impressive 23-fold in cases in which ruptured plaque was identified compared with a thick fibrous cap. These encouraging observations will pave the way for studies that prospectively examine plaque behavior.

### Coronary Artery Imaging

Recently, coronary arteries have been imaged in vivo by MRI (Figure 2).<sup>34,55,56,60</sup> Coronary imaging poses considerable technical difficulties. The coronary arteries are relatively small and have a tortuous and unpredictable course. In addition, to obtain MR images, cardiac and respiratory motion must be overcome. Use of MR navigator echoes that assess cardiac or diaphragmatic position accounts for movement and eliminates the time constraint imposed by imaging in a single breath-holding, as shown in a recent multicenter study of coronary MR angiography.<sup>61</sup> This provides longer effective image acquisition to enable submillimeter spatial resolution (Botnar et al<sup>55</sup>). Botnar et al<sup>60</sup> have further refined their 3D coronary wall imaging technique by the application of a local inversion technique, improving contrast between lumen and vessel wall in a series of normal subjects and attaining a resolution of  $0.66 \times 0.66 \times 2 \text{ mm}^3$ .<sup>60</sup> Current coronary MRI techniques have limited spatial resolution mainly because of the available signal-to-noise ratio. One way to increase the signal-to-noise ratio directly is to improve the

**TABLE 1. MRI Parameters in Selected Cited Studies**

Species	Setting	Magnet, T	Contrast Weighting	TR/TE, ms/ms	Voxel, $\mu\text{m}$	Time	Reference
Xenopus	In vivo embryo	11.7	3D-spin echo-T1W	400/21	27 $\times$ 16 $\times$ 16	3 h 45 min	Louie, 2000 <sup>133</sup>
Mouse	In vivo tumor	1.5	T1W, T2W	na	300 $\times$ 300 $\times$ 700	3–7 min	Weissleder, 2000 <sup>132</sup>
Mouse	Ex vivo tumor	7.1	T1W, T2W	na	39 $\times$ 39 $\times$ 39	5.5 h	Weissleder, 2000 <sup>132</sup>
Mouse	Ex vivo brain	9.4	T1W	200/4	40 $\times$ 40 $\times$ 40	7 h	Sipkins, 2000 <sup>137</sup>
Mouse	In vivo aorta	9.4	T2W	2000/30	48 $\times$ 48 $\times$ 500	17 min	Fayad, 1998 <sup>27</sup>
			PDW	2000/13			
Rabbit	In vivo aorta	1.5	T2W	2300/60	35 $\times$ 35 $\times$ 3000	70 min	Heftt, 2001 <sup>30</sup>
			PDW	2300/17			
Pig	In vivo coronary	1.5	T2W	2 RR'/42	390 $\times$ 390 $\times$ 500	na	Worthley, 2000 <sup>28</sup>
			PDW	2 RR'/17			
Human	In vivo carotid	1.5	T2W	1 RR'/20 & 55	390 $\times$ 390 $\times$ 5000	na	Toussaint, 1996 <sup>33</sup>
Human	In vivo carotid	1.5	MOTSA-T1W	34; 22/2.9; 4.4	254 $\times$ 254 $\times$ 1000	1–5 min	Hatsukami, 2000 <sup>53</sup>
Human	In vivo coronary	1.5	T2W	2 RR'/25	500 $\times$ 1000 $\times$ 5000	na	Botnar, 2000 <sup>56</sup>
Human	In vivo coronary	1.5	T2W, BBI	2 RR'/40	460 $\times$ 460 $\times$ 3000	1 BH	Fayad, 2000 <sup>34</sup>

RR' indicates R-R' interval measured from electrocardiogram; MOTSA, multiple-overlapping thin-slab angiography; BBI, black blood imaging; BH, breath hold; na, data unavailable; TR, repetition time; TE, echo time.

receiver coils. This has been shown by Fayad et al,<sup>62</sup> who used a 4-element anterior phased-array coil that enabled in a series of patients in vivo coronary wall imaging at a resolution of 0.39 $\times$ 0.39 $\times$ 2 mm<sup>3</sup>. This in-plane resolution was found to be adequate in providing an accurate (measurement error <20%) assessment of the “normal” and diseased vessel wall area, as shown by numerical simulations and phantom measurements.<sup>63</sup>

Acquisition of isotropic voxels, which facilitate reconstruction of the coronary arteries in arbitrary and exhaustive views,<sup>64</sup> may compensate for the problem of tortuosity.

MRI characterization of human coronary atherosclerotic plaque components has been demonstrated ex vivo.<sup>65</sup> Although not yet accomplished, there is well-founded optimism<sup>63</sup> that in vivo human coronary plaque characterization will be attainable relatively soon.

## Plaque and Thrombus Characterization With Use of Contrast Agents

### Plaque Characterization

The characterization techniques described above use the inherent relaxation properties of different plaque components. Despite the use of multispectral MR<sup>58</sup> or of high (200- $\mu\text{m}^3$ ) resolution in 3D imaging,<sup>66</sup> it has still not been possible to identify uniquely plaque components. An overlap of signal intensities occurs, particularly between the lipid core and vessel media.<sup>58,66</sup> Moreover, approaches that are directed at the identification of the lipid core and fibrous cap are focused on relatively advanced lesions. More subtle distinctions within plaque and preatheromatous artery may be detectable by the introduction of paramagnetic contrast agents, such as gadolinium.

**TABLE 2. Specific Contrast Agents Used in Selected Cited Studies**

Species	Setting	Target	Contrast Agent	Contrast Weighting	Magnet, T	Reference
Human	Aorto-iliac plaque	Neovasculature	MS-325 (Gd)	$\uparrow$ (T1W)	1.5	Maki 2001 <sup>75</sup>
Human	Carotid plaque	Neovasculature	Omniscan (Gd)	$\uparrow$ (T1W)	1.5	Yuan 2001 <sup>73</sup>
Rabbit	Aortic plaque	Macrophages	SPIO	$\downarrow$ (T2W)	1.5	Schmitz 2001 <sup>79</sup>
Rabbit	Aortic plaque	Macrophages	USPIO	$\downarrow$ (T1W)	1.5	Ruehm 2001 <sup>78</sup>
Pig	Venous thrombus	$\alpha_{\text{IIb}}\beta_3$ integrin	RGD-USPIO	$\uparrow$ (T1W)	1.5	Johansson 2001 <sup>91</sup>
Ex-vivo	Thrombus	Fibrin	ACPL (Gd)	$\downarrow$ (T1/2W)	4.7	Yu 2000 <sup>88</sup>
Rabbit	Tumor angiogenesis	$\alpha_v\beta_3$ integrin	ACPL (Gd)	$\uparrow$ (T1W)	1.5	Sipkins 1998 <sup>138</sup>
Rabbit	Corneal angiogenesis	$\alpha_v\beta_3$ integrin	ACPL (Gd)	$\uparrow$ (T1W)	4.7	Anderson 2000 <sup>139</sup>
Mouse	Tumor	Transferrin receptor (transgenic)	Tf-MION	$\downarrow$ (T1/2W)	7.1	Weissleder 2000 <sup>132</sup>
Mouse	Encephalitis	ICAM-1	ACPL (Gd)	$\uparrow$ (T1W)	9.4	Sipkins 2000 <sup>137</sup>
Xenopus	Embryonic gene expression	$\beta$ -galactosidase activity	E-gadMe	$\uparrow$ (T1W)	9.4	Louie 2000 <sup>133</sup>

ACPL indicates antibody-conjugated paramagnetic liposome; E-GadMe, (1-(2- $\beta$ -galactopyranosyloxy)propyl)-4,7,10-tris(carboxymethyl)-1,4,7,10-tetraazacyclododecane)gadolinium(III); Gd, gadolinium-based contrast agent; ICAM-1, intercellular adhesion molecule 1; Tf-MION, human transferrin receptor–low-molecular weight-dextran–monocrystalline iron oxide nanoparticle complex; RGD-SPIO, arginine-glycine-aspartic acid peptide-SPIO conjugate; (U)SPIO, (ultra-small) superparamagnetic particles of iron oxide.

Gadolinium chelates enhance T1 relaxation and, therefore, increase contrast enhancement on T1W pulse sequences with short repetition times and echo times.<sup>67</sup> For the purposes of MR angiography, gadolinium has been used to improve blood-tissue contrast,<sup>68</sup> but it can potentially enhance the contrast in any tissue in which it resides. New microvessels form in atherosclerotic plaque, and these may be associated with features of inflammation, such as upregulation of adhesion molecules and leukocyte infiltration.<sup>69</sup> The presence of new vessels has also been associated with carotid plaque instability.<sup>70</sup> These vessels may also be abnormally permeable, allowing the extravasation of plasma proteins, such as albumin and fibrinogen.<sup>71,72</sup> In recent reports, contrast MRI has used these features to aid plaque characterization. On T1W images of carotid arteries, a gadolinium-based contrast agent has been reported to differentially enhance areas rich in plaque microvascularization and may offer a further means of distinguishing the necrotic core and fibrous cap and of highlighting at-risk plaque.<sup>73</sup> By use of MS-325, a gadolinium-based contrast agent that binds albumin, areas of high signal intensity, comparable to highly vascular tissue such as liver, have been observed in the aortic or iliac arterial wall. It has been speculated that this reflects not only increased plaque vascularity<sup>74</sup> but also a leakiness of these microvessels, which suggests active inflammation.<sup>75</sup> This is consistent with a recent report in which increased wall thickness, T2W signal, and/or gadolinium contrast enhancement in carotid arteries and aorta was associated with elevated serum levels of the inflammatory markers interleukin-6, C-reactive protein, intercellular adhesion molecule-1, and vascular cell adhesion molecule-1.<sup>76</sup>

Contrast agents that specifically identify components of vulnerable plaque are of considerable interest. Macrophage-rich areas are a pathological correlate of unstable plaque.<sup>42</sup> Superparamagnetic nanoparticles of iron oxide (SPIO) alter the MRI reaction times and are taken up avidly by macrophages. In recent small studies, injection of SPIO into hyperlipidemic rabbits was associated with accumulation in macrophages and, after 2 hours<sup>77</sup> to 5 days,<sup>78</sup> the appearance of signal voids studded on the luminal surface of the aorta. Similar appearances have been observed incidentally in the aorta and intrapelvic arteries of humans that have received SPIO for oncological imaging.<sup>79</sup> This type of specific cellular targeting approach warrants further investigation.

### Thrombus Characterization

Plaque rupture or erosion exposes the prothrombotic core to circulating blood,<sup>10,21</sup> which can lead to acute vessel occlusion and myocardial infarction, unstable angina, or death. Recent evidence suggests that layering and organization of the thrombus may be responsible for plaque progression.<sup>23</sup> Johnstone et al<sup>80</sup> have identified the location and size of plaque-associated mural thrombus in vivo in an atherosclerotic rabbit model.<sup>80</sup> Rapid noninvasive identification and age characterization of the thrombus may be clinically useful (eg, if treatment risk versus benefit is related to the timing and location of a thrombotic event). Time-related changes in the water-diffusion properties of the thrombus have been identified by using pulse-field gradient methods.<sup>81</sup> MR signal

intensities of hemorrhage and “altered blood” depend on the structure of hemoglobin and its oxidation state.<sup>82</sup> For example, the generation of methemoglobin within an evolving thrombus is known to cause T1 shortening. This phenomenon has been exploited for the detection of fresh thrombus in the setting of deep vein thrombosis,<sup>83,84</sup> pulmonary embolus,<sup>85</sup> and acute carotid thrombus.<sup>74</sup> In these studies, direct imaging of the thrombus against a suppressed background with the use of a 3D magnetization-prepared rapid gradient echo<sup>86</sup> has been found to be effective in the imaging of thrombi.

The potential of MRI to detect arterial thrombotic obstruction and define thrombus age has been very recently evaluated by using black-blood T1W and T2W.<sup>87</sup> Carotid thrombi were induced in swine by arterial injury. Serial high-resolution in vivo MR images were obtained at 6 hours, at 1 day, and at 1, 2, 3, 6, and 9 weeks. Thrombus appearance and relative signal intensity revealed characteristic temporal changes in the MR images, reflecting histological changes in the composition. Age definition using visual appearance was highly accurate (Pearson  $\chi^2$  with 4 *df* ranging from 96 to 132 and Cohen  $\kappa$  0.81 to 0.94).

Contrast agents that characterize thrombi are under development: fibrin can be identified by lipid-encapsulated perfluorocarbon paramagnetic nanoparticles in vitro<sup>88,89</sup> and in vivo<sup>89</sup> or by a paramagnetic dendrimeric contrast agent,<sup>90</sup> whereas activated platelets can be targeted via the interaction of an ultrasmall SPIO-arginine-glycine-aspartic acid (RGD) peptide construct with the  $\alpha_{IIb}\beta_3$  receptor (Table 2).<sup>91</sup>

### Effects of Treatment

Direct plaque imaging is of potential use not only for diagnosis but also for monitoring response to treatment. Angiographic studies of progression and regression of atherosclerosis have been notoriously poor at demonstrating changes in plaque burden, even when changes in clinical event rates have been markedly altered.<sup>92,93</sup> In a study of diet/injury-induced atherosclerosis in rabbits, T2W MRI identified regression of atherosclerosis 12 to 20 months after the withdrawal of the atherogenic diet (regression group). In contrast, lesion progression was documented in rabbits that continued the atherogenic diet (progression group).<sup>94</sup> Morphometric data were presented as changes in wall thickness and percent stenosis (separate values for wall area and lumen area were not given in the study). In a similar study,<sup>95</sup> serial MRI showed a significant reduction in the lipid components of the plaque in the regression group and an increase in the progression group.

In a preliminary analysis, using PDW and T2W MRI, Corti et al<sup>35</sup> illustrated a decrease in cross-sectional wall area in atherosclerotic segments of human aorta and carotid artery (by 8% and 15%, respectively) 12 months after the initiation of simvastatin. Importantly, there was no change in cross-sectional area of the arterial lumen. This emphasizes the importance of imaging the vessel wall directly and probably explains the limitations of coronary angiography in assessing response to treatment. In another recent case-control study, 8 patients with coronary artery disease who were subjected to prolonged intensive lipid-lowering (niacin, lovastatin, and colestipol over 10 years) showed a dramatic reduction

(0.7 mm<sup>2</sup> versus 10.9 mm<sup>2</sup>,  $P < 0.001$ ) in plaque lipid content.<sup>96</sup> In that small study, differences between the groups in overall plaque area and lumen area did not reach statistical significance.

### Image Analysis

As demonstrated above, a significant strength of MRI is the ability, noninvasively, to follow the progress of lesions in individual patients over a period of time. Comparisons of this nature will provide insight into the natural history of plaque and prospective information about plaque at risk of precipitating an acute atherothrombotic event, and they will also provide information regarding response to treatment. However, changes in plaque size and composition within individuals may be small.<sup>35,96</sup> Reliable ways to ensure anatomic alignment of sections between successive scans and to measure small changes in measured parameters are required.

In our lipid-lowering study of human aortic and carotid plaques,<sup>35</sup> the reproducibility of the vessel wall area measurement was assessed after repeated imaging. The error in vessel wall area measurement was found to be 2.6% for aortic plaque and 3.5% for carotid plaque. Similar low measurement errors in plaque area and volume (4% to 6%) have been reported by others, proving that plaque area and volume can be accurately assessed.<sup>97,98</sup>

To improve quantification, semiautomatic image-processing techniques have been developed that improve the accuracy of vessel wall area measurements compared with the accuracy provided by manual morphometric analysis.<sup>99,100</sup> In one such model, a “discrete dynamic contour” is produced by image-derived edge characteristics moderated by elements to introduce contour tension and damping. Three-dimensional interpolation of discrete dynamic contours attained for inner and outer vessel walls has allowed construction of vessel wall volume,<sup>101</sup> with the potential to quantify atherosclerotic plaque burden and distribution.

### Vascular Intervention

High-resolution images of vessel wall, excellent delineation of perivascular soft tissue structures, inherent versatility of multiple plane viewing, virtual real-time images, and the ability to acquire angiographic and hemodynamic data make MRI an exceptionally promising platform for intravascular intervention.<sup>102</sup>

Preliminary studies have indicated the feasibility of MR-guided percutaneous angioplasty in rabbit aorta,<sup>103</sup> of stent deployment in pig femoral arteries,<sup>104</sup> rabbit aortas,<sup>105</sup> and pig coronary arteries,<sup>106</sup> and of the monitoring of catheter-based gene therapy in pig femoral arteries.<sup>107</sup> In humans, intraoperative MR has been shown to be safe and effective for intracranial neurosurgery,<sup>108</sup> although transvascular applications are, thus far, limited.<sup>109</sup> MR-guided coronary intervention is a relatively distant but attainable objective.

### Emerging MRI Applications and Molecular Mechanisms

#### MRI in Transgenic Mouse Models of Atherosclerosis

Mouse models have largely superseded larger animal models of human atherosclerosis (Figure 4).<sup>110–113</sup> Mice have the

advantages of small size, ample progeny, and a short reproductive cycle. Genetically modified mice spontaneously and reproducibly develop atherosclerosis that resembles that found in humans.<sup>114,115</sup> In addition, characterization of the mouse genome has enabled the application of gene knockout and transgenic technologies to study the progression<sup>116–119</sup> and regression<sup>120–123</sup> of atherosclerosis. Despite these advantages, a significant drawback of the study of such small animals has been the inability to track the progression or regression of atherosclerosis *in vivo*.<sup>124</sup>

We have previously demonstrated that MR can accurately quantify atherosclerosis in apoE-deficient mice.<sup>27</sup> By imaging at 9.4 T, with an in-plane resolution of 100×100 μm, the progression of atherosclerosis can be identified in individual mice,<sup>125</sup> and the progression of atherosclerosis can be shown to be accompanied by positive arterial remodeling.<sup>126</sup>

In these studies, atherosclerosis was quantified in the abdominal aorta. Carotid artery imaging after wire injury has also been performed in mice.<sup>127</sup> Respiratory and cardiac gating and continuous anesthetic administration will allow extended imaging to improve image quality<sup>128,129</sup> and will enable imaging of the thoracic aorta and aortic root. The aortic root is an attractive location for imaging because lesions develop earlier there than in the abdominal aorta. Furthermore, pathological studies of atherosclerosis in mice have been largely standardized to examine the aortic root.<sup>116,130</sup>

#### MRI and Molecular Imaging

The ability to image the presence or activity of specific molecules *in vivo* (Table 2) would be of considerable interest.<sup>131</sup> MRI can achieve spatial resolution to ≈10 μm. This capability exceeds that of positron emission tomography, single positron emission CT, and nuclear techniques.

Weissleder et al<sup>132</sup> have refined and extended the application of superparamagnetic contrast through transgenic expression of transferrin receptor in nude mice. The resultant increase of the uptake of injected superparamagnetic iron nanoparticles significantly decreased the MR signal in a tumor model, relative to transferrin receptor-negative controls, such that the expression of the transgene could be mapped noninvasively by the use of MRI.

Louie et al<sup>133</sup> have developed an MR contrast agent capable of reporting the activity of a β-galactosidase. The paramagnetic agent (abbreviated EgadMe) requires interaction with a water molecule to generate an increased MR signal in T1W images. In the resting state, however, its interaction with water is prevented by the attachment of galactopyranose, a “blocking group” that is susceptible to enzymatic cleavage by β-galactosidase. The subsequent association of water with EgadMe results in an increase of T1 signal by ≈60%. By use of this approach, it was possible to localize the lineage of a cell injected with β-galactosidase mRNA in early embryonic development. The ability to image areas in which β-galactosidase is active may be of considerable use in the study of transgenic animals and in mapping sites of expression *in vivo* in gene therapy. Moreover, this technique may represent a paradigm of intelligent contrast agents that are activated in response to specific biological

events. EganMe and its successors may be conjugated with blocking units that are substrates for other enzymes. In the context of atherosclerosis, matrix metalloproteinases (MMPs) digest collagen, elastin, and other matrix components. Some MMPs are believed to be important in the generation of unstable plaque<sup>20</sup>; thus, identification of vulnerable plaque may be feasible by targeting specific proteolytic activities. MMPs have the additional advantage of extracellular activity, thus circumventing the problem of intracellular access by contrast agents.

The endothelial cell surface proteins, vascular cell adhesion molecule-1 and intercellular adhesion molecule-1, are upregulated in atherosclerotic plaque<sup>134,135</sup> and in areas of artery prone to lesion formation.<sup>136</sup> Exposure to circulating blood renders such molecules potential targets for monoclonal antibody-conjugated intravascular MR contrast agents. Antibodies conjugated to paramagnetic liposomes have been used to image, *ex vivo*, intercellular adhesion molecule expression in a murine model of multiple sclerosis<sup>137</sup> and  $\alpha_v\beta_3$  integrin expression as a marker of angiogenesis.<sup>138,139</sup> Where cells are accessible to blood, perhaps as a consequence of abnormal vascular permeability in plaques, imaging specific receptor expression with the use of contrast-ligand constructs should also be feasible.<sup>140</sup>

### Conclusions

In the future, clinical investigation of atherosclerosis will not be restricted by the endoluminal approach that has limited x-ray contrast arteriography. High-resolution noninvasive MRI will provide exhaustive 3D anatomic information about the lumen and the vessel wall. Furthermore, MRI has the ability to characterize plaque composition and microanatomy and, therefore, to identify lesions vulnerable to rupture or erosion. This may aid in early intervention in the primary and secondary treatment of vascular disease. The high resolution of MRI and the development of sophisticated contrast agents offer the promise of molecular *in vivo* molecular imaging of the plaque.

### Acknowledgments

Partial support for this study was provided by National Institutes of Health grants HL-61801 (V.F., Z.A.F., J.J.B.) and HL-61814 (E.A.F., Z.A.F.), by the Howard Hughes Medical Institute Biomedical Support Program (Z.A.F.), and by the New York Community Trust (Z.A.F.). R.P.C. holds a Wellcome Trust International Fellowship. We thank Drs Roberto Corti, Gilbert J. Aguinaldo, and Rachel R. Phillips for their contributions. Victoria Wei is acknowledged for technical help.

### References

1. Fariñas PL. A new technique for the arteriographic examination of the abdominal aorta and its branches. *AJR Am J Roentgenol.* 1941;46:641–645.
2. Mueller RL, Sanborn TA. The history of interventional cardiology: cardiac catheterization, angioplasty, and related interventions. *Am Heart J.* 1995;129:146–172.
3. Holmes DR Jr, Vlietstra RE, Fisher LD, Smith HC, Mock MB, Faxon DP, Gosselin AJ, Ryan TJ, Judkins MP, Pettinger M. Follow-up of patients from the coronary artery surgery study (CASS) potentially suitable for percutaneous transluminal coronary angioplasty. *Am Heart J.* 1983;106:981–988.
4. Kennedy JW, Killip T, Fisher LD, Alderman EL, Gillespie MJ, Mock MB. The clinical spectrum of coronary artery disease and its surgical

- and medical management, 1974–1979: the Coronary Artery Surgery study. *Circulation.* 1982;66(suppl III):III-16–III-23.
5. Serruys PW, Unger F, Sousa JE, Jatene A, Bonnier HJ, Schonberger JP, Buller N, Bonser R, van den Brand MJ, van Herwerden LA, Morel MA, van Hout BA. Comparison of coronary-artery bypass surgery and stenting for the treatment of multivessel disease. *N Engl J Med.* 2001;344:1117–1124.
6. Glagov S, Weisenberg E, Zarins CK, Stankunavicius R, Kolettis GJ. Compensatory enlargement of human atherosclerotic coronary arteries. *N Engl J Med.* 1987;316:1371–1375.
7. Ward MR, Pasterkamp G, Yeung AC, Borst C. Arterial remodeling: mechanisms and clinical implications. *Circulation.* 2000;102:1186–1191.
8. Ambrose JA, Tannenbaum MA, Alexopoulos D, Hjemdahl-Monsen CE, Leavy J, Weiss M, Borrico S, Gorlin R, Fuster V. Angiographic progression of coronary artery disease and the development of myocardial infarction. *J Am Coll Cardiol.* 1988;12:56–62.
9. Little WC, Constantinescu M, Applegate RJ, Kutcher MA, Burrows MT, Kahl FR, Santamore WP. Can coronary angiography predict the site of a subsequent myocardial infarction in patients with mild-to-moderate coronary artery disease? *Circulation.* 1988;78:1157–1166.
10. Falk E, Shah PK, Fuster V. Coronary plaque disruption. *Circulation.* 1995;92:657–671.
11. Fuster V, Fayad ZA, Badimon JJ. Acute coronary syndromes: biology. *Lancet.* 1999;353(suppl 2):SII5–SII9.
12. Hansson GK. The stabilized plaque: will the dream come true? *Eur Heart J.* 2001;3:C69–C75.
13. Rumberger JA. Tomographic (plaque) imaging: state of the art. *Am J Cardiol.* 2001;88:66E–69E.
14. Fayad ZA, Fuster V. Clinical imaging of the high-risk or vulnerable atherosclerotic plaque. *Circ Res.* 2001;89:305–316.
15. Hennerici M, Meairs S. Imaging arterial wall disease. *Cerebrovasc Dis.* 2000;10(suppl 5):9–20.
16. Pathobiological Determinants of Atherosclerosis in Youth (PDAY) Research Group. Natural history of aortic and coronary atherosclerotic lesions in youth: findings from the PDAY Study. *Arterioscler Thromb.* 1993;13:1291–1298.
17. Shepherd J, Cobbe SM, Ford I, Isles CG, Lorimer AR, MacFarlane PW, McKillop JH, Packard CJ. Prevention of coronary heart disease with pravastatin in men with hypercholesterolemia: West of Scotland Coronary Prevention Study Group. *N Engl J Med.* 1995;333:1301–1307.
18. Downs JR, Clearfield M, Weis S, Whitney E, Shapiro DR, Beere PA, Langendorfer A, Stein EA, Krueyer W, Gotto AM Jr. Primary prevention of acute coronary events with lovastatin in men and women with average cholesterol levels: results of AFCAPS/TexCAPS: Air Force/Texas Coronary Atherosclerosis Prevention Study. *JAMA.* 1998;279:1615–1622.
19. Executive Summary of The Third Report of The National Cholesterol Education Program (NCEP) Expert Panel on Detection, Evaluation, and Treatment of High Blood Cholesterol in Adults (Adult Treatment Panel III). *JAMA.* 2001;285:2486–2497.
20. Galis ZS, Sukhova GK, Lark MW, Libby P. Increased expression of matrix metalloproteinases and matrix degrading activity in vulnerable regions of human atherosclerotic plaques. *J Clin Invest.* 1994;94:2493–2503.
21. Farb A, Burke AP, Tang AL, Liang TY, Mannan P, Smialek J, Virmani R. Coronary plaque erosion without rupture into a lipid core: a frequent cause of coronary thrombosis in sudden coronary death. *Circulation.* 1996;93:1354–1363.
22. Aikawa M, Rabkin E, Okada Y, Voglic SJ, Clinton SK, Brinckerhoff CE, Sukhova GK, Libby P. Lipid lowering by diet reduces matrix metalloproteinase activity and increases collagen content of rabbit atheroma: a potential mechanism of lesion stabilization. *Circulation.* 1998;97:2433–2444.
23. Virmani R, Kolodgie FD, Burke AP, Farb A, Schwartz SM. Lessons from sudden coronary death: a comprehensive morphological classification scheme for atherosclerotic lesions. *Arterioscler Thromb Vasc Biol.* 2000;20:1262–1275.
24. Skinner MP, Yuan C, Mitsumori L, Hayes CE, Raines EW, Nelson JA, Ross R. Serial magnetic resonance imaging of experimental atherosclerosis detects lesion fine structure, progression and complications *in vivo*. *Nat Med.* 1995;1:69–73.
25. Kaneko E, Yuan C, Skinner MP, Raines EW, Ross R. Serial magnetic resonance imaging of experimental atherosclerosis allows visualization of lesion characteristics and lesion progression *in vivo*. *Ann NY Acad Sci.* 1997;811:245–252.

26. Yuan C, Beach KW, Smith LH Jr, Hatsukami TS. Measurement of atherosclerotic carotid plaque size in vivo using high resolution magnetic resonance imaging. *Circulation.* 1998;98:2666–2671.
27. Fayad ZA, Fallon JT, Shinnar M, Wehrli S, Dansky HM, Poon M, Badimon JJ, Charlton SA, Fisher EA, Breslow JL, Fuster V. Noninvasive in vivo high-resolution magnetic resonance imaging of atherosclerotic lesions in genetically engineered mice. *Circulation.* 1998;98:1541–1547.
28. Worthley SG, Helft G, Fuster V, Fayad ZA, Rodriguez OJ, Zaman AG, Fallon JT, Badimon JJ. Noninvasive in vivo magnetic resonance imaging of experimental coronary artery lesions in a porcine model. *Circulation.* 2000;101:2956–2961.
29. Worthley SG, Helft G, Fuster V, Zaman AG, Fayad ZA, Fallon JT, Badimon JJ. Serial in vivo MRI documents arterial remodeling in experimental atherosclerosis. *Circulation.* 2000;101:586–589.
30. Helft G, Worthley SG, Fuster V, Zaman AG, Schechter C, Osende JJ, Rodriguez OJ, Fayad ZA, Fallon JT, Badimon JJ. Atherosclerotic aortic component quantification by noninvasive magnetic resonance imaging: an in vivo study in rabbits. *J Am Coll Cardiol.* 2001;37:1149–1154.
31. Herfkens RJ, Higgins CB, Hricak H, Lipton MJ, Crooks LE, Sheldon PE, Kaufman L. Nuclear magnetic resonance imaging of atherosclerotic disease. *Radiology.* 1983;148:161–166.
32. Merickel MB, Berr S, Spetz K, Jackson TR, Snell J, Gillies P, Shimshick E, Hainer J, Brookeman JR, Ayers CR. Noninvasive quantitative evaluation of atherosclerosis using MRI and image analysis. *Arterioscler Thromb.* 1993;13:1180–1186.
33. Toussaint JF, LaMuraglia GM, Southern JF, Fuster V, Kantor HL. Magnetic resonance images lipid, fibrous, calcified, hemorrhagic, and thrombotic components of human atherosclerosis in vivo. *Circulation.* 1996;94:932–938.
34. Fayad ZA, Fuster V, Fallon JT, Jayasundera T, Worthley SG, Helft G, Aguinaldo JG, Badimon JJ, Sharma SK. Noninvasive in vivo human coronary artery lumen and wall imaging using black-blood magnetic resonance imaging. *Circulation.* 2000;102:506–510.
35. Corti R, Fayad ZA, Fuster V, Worthley SG, Helft G, Chesebro J, Mercuri M, Badimon JJ. Effects of lipid-lowering by simvastatin on human atherosclerotic lesions: a longitudinal study by high-resolution, noninvasive magnetic resonance imaging. *Circulation.* 2001;104:249–252.
36. Wood ML, Wehrli FW. Principles of magnetic resonance imaging. In: Stark DD, Bradley WG Jr, eds. *Magnetic Resonance Imaging.* St Louis, Mo: Mosby; 1999.
37. Mitchell DG. *MRI Principles.* Philadelphia, Pa: Saunders; 1999.
38. Doyle M, Pohost GM. Magnetic resonance imaging of the heart. In: Fuster V, Alexander RW, O'Rourke RA, eds. *Hurst's The Heart.* New York, NY: McGraw Hill; 2000.
39. von Birgelen C, Klinkhart W, Mintz GS, Papatheodorou A, Herrmann J, Baumgart D, Haude M, Wieneke H, Ge J, Erbel R. Plaque distribution and vascular remodeling of ruptured and nonruptured coronary plaques in the same vessel: an intravascular ultrasound study in vivo. *J Am Coll Cardiol.* 2001;37:1864–1870.
40. Shah PK, Falk E, Badimon JJ, Fernandez-Ortiz A, Mailhac A, Villareal-Levy G, Fallon JT, Regnstrom J, Fuster V. Human monocyte-derived macrophages induce collagen breakdown in fibrous caps of atherosclerotic plaques: potential role of matrix-degrading metalloproteinases and implications for plaque rupture. *Circulation.* 1995;92:1565–1569.
41. Davies MJ, Richardson PD, Woolf N, Katz DR, Mann J. Risk of thrombosis in human atherosclerotic plaques: role of extracellular lipid, macrophage, and smooth muscle cell content. *Br Heart J.* 1993;69:377–381.
42. Moreno PR, Falk E, Palacios IF, Newell JB, Fuster V, Fallon JT. Macrophage infiltration in acute coronary syndromes: implications for plaque rupture. *Circulation.* 1994;90:775–778.
43. Libby P, Geng YJ, Aikawa M, Schoenbeck U, Mach F, Clinton SK, Sukhova GK, Lee RT. Macrophages and atherosclerotic plaque stability. *Curr Opin Lipidol.* 1996;7:330–335.
44. Richardson PD, Davies MJ, Born GV. Influence of plaque configuration and stress distribution on fissuring of coronary atherosclerotic plaques. *Lancet.* 1989;2:941–944.
45. Mohiaddin RH, Firmin DN, Underwood SR, Abdulla AK, Klipstein RH, Rees RS, Longmore DB. Chemical shift magnetic resonance imaging of human atheroma. *Br Heart J.* 1989;62:81–89.
46. Vinitski S, Consigny PM, Shapiro MJ, Janes N, Smullens SN, Rifkin MD. Magnetic resonance chemical shift imaging and spectroscopy of atherosclerotic plaque. *Invest Radiol.* 1991;26:703–714.
47. Small DM. George Lyman Duff memorial lecture: progression and regression of atherosclerotic lesions: insights from lipid physical biochemistry. *Arteriosclerosis.* 1988;8:103–129.
48. Toussaint JF, Southern JF, Fuster V, Kantor HL. <sup>13</sup>C-NMR spectroscopy of human atherosclerotic lesions: relation between fatty acid saturation, cholesteryl ester content, and luminal obstruction. *Arterioscler Thromb.* 1994;14:1951–1957.
49. Trouard TP, Altbach MI, Hunter GC, Eskelson CD, Gmitro AF. MRI and NMR spectroscopy of the lipids of atherosclerotic plaque in rabbits and humans. *Magn Reson Med.* 1997;38:19–26.
50. Toussaint JF, Southern JF, Fuster V, Kantor HL. T<sub>2</sub>-weighted contrast for NMR characterization of human atherosclerosis. *Arterioscler Thromb Vasc Biol.* 1995;15:1533–1542.
51. Pearlman JD, Zajicek J, Merickel MB, Carman CS, Ayers CR, Brookeman JR, Brown MF. High-resolution <sup>1</sup>H NMR spectral signature from human atheroma. *Magn Reson Med.* 1988;7:262–279.
52. Shinnar M, Fallon JT, Wehrli S, Levin M, Dalmacy D, Fayad ZA, Badimon JJ, Harrington M, Harrington E, Fuster V. The diagnostic accuracy of ex vivo MRI for human atherosclerotic plaque characterization. *Arterioscler Thromb Vasc Biol.* 1999;19:2756–2761.
53. Hatsukami TS, Ross R, Polissar NL, Yuan C. Visualization of fibrous cap thickness and rupture in human atherosclerotic carotid plaque in vivo with high-resolution magnetic resonance imaging. *Circulation.* 2000;102:959–964.
54. Fayad ZA, Nahar T, Fallon JT, Goldman M, Aguinaldo JG, Badimon JJ, Shinnar M, Chesebro JH, Fuster V. In vivo magnetic resonance evaluation of atherosclerotic plaques in the human thoracic aorta: a comparison with transesophageal echocardiography. *Circulation.* 2000;101:2503–2509.
55. Botnar RM, Stuber M, Danias PG, Kissinger KV, Manning WJ. Improved coronary artery definition with T<sub>2</sub>-weighted, free-breathing, three-dimensional coronary MRA. *Circulation.* 1999;99:3139–3148.
56. Botnar RM, Stuber M, Kissinger KV, Kim WY, Spuentrup E, Manning WJ. Noninvasive coronary vessel wall and plaque imaging with magnetic resonance imaging. *Circulation.* 2000;102:2582–2587.
57. Yuan C, Mitsumori LM, Beach KW, Maravilla KR. Carotid atherosclerotic plaque: noninvasive MR characterization and identification of vulnerable lesions. *Radiology.* 2001;221:285–299.
58. Yuan C, Mitsumori LM, Ferguson MS, Polissar NL, Echelard D, Ortiz G, Small R, Davies JW, Kerwin WS, Hatsukami TS. In vivo accuracy of multispectral magnetic resonance imaging for identifying lipid-rich necrotic cores and intraplaque hemorrhage in advanced human carotid plaques. *Circulation.* 2001;104:2051–2056.
59. Yuan C, Zhang SX, Polissar NL, Echelard D, Ortiz G, Davis JW, Ellington E, Ferguson MS, Hatsukami TS. Identification of fibrous cap rupture with magnetic resonance imaging is highly associated with recent transient ischemic attack or stroke. *Circulation.* 2002;105:181–185.
60. Botnar RM, Kim WY, Bornert P, Stuber M, Spuentrup E, Manning WJ. 3D coronary vessel wall imaging utilizing a local inversion technique with spiral image acquisition. *Magn Reson Med.* 2001;46:848–854.
61. Kim WY, Danias PG, Stuber M, Flamm SD, Plein S, Nagel E, Langerak SE, Weber OM, Pedersen EM, Schmidt M, Botnar RM, Manning WJ. Coronary magnetic resonance angiography for the detection of coronary stenoses. *N Engl J Med.* 2001;345:1863–1869.
62. Fayad ZA, Hardy CJ, Giaquinto R, Kini A, Sharma S. Improved high resolution MRI of human coronary lumen and plaque with a new cardiac coil. *Circulation.* 2000;102(suppl II):II-399. Abstract.
63. Schär M, Kim WY, Stuber M, Boesiger P, Manning WJ, Botnar RM. The impact of spatial resolution and respiratory motion on magnetic resonance plaque characterization. *J Cardiovasc Magn Reson.* 2002;4:73. Abstract.
64. Botnar RM, Stuber M, Kissinger KV, Manning WJ. Free-breathing 3D coronary MRA: the impact of isotropic image resolution. *J Magn Reson Imaging.* 2000;11:389–393.
65. Yuan C, Hatsukami TS, Obrien KD. High-resolution magnetic resonance imaging of normal and atherosclerotic human coronary arteries ex vivo: discrimination of plaque tissue components. *J Investig Med.* 2001;49:491–499.
66. Coombs BD, Rapp JH, Ursell PC, Reilly LM, Saloner D. Structure of plaque at carotid bifurcation: high-resolution MRI with histological correlation. *Stroke.* 2001;32:2516–2521.

67. Runge VM, Nelson KM. Contrast Agents. In: Stark DD, Bradley WG, eds. *Magnetic Resonance Imaging*. St Louis, Mo: Mosby; 1999.
68. Regenfus M, Ropers D, Achenbach S, Kessler W, Laub G, Daniel WG, Moshage W. Noninvasive detection of coronary artery stenosis using contrast-enhanced three-dimensional breath-hold magnetic resonance coronary angiography. *J Am Coll Cardiol*. 2000;36:44–50.
69. de Boer OJ, van der Wal AC, Teeling P, Becker AE. Leucocyte recruitment in rupture prone regions of lipid-rich plaques: a prominent role for neovascularization? *Cardiovasc Res*. 1999;41:443–449.
70. McCarthy MJ, Loftus IM, Thompson MM, Jones L, London NJ, Bell PR, Naylor AR, Brindle NP. Angiogenesis and the atherosclerotic carotid plaque: an association between symptomatology and plaque morphology. *J Vasc Surg*. 1999;30:261–268.
71. Zhang Y, Cliff WJ, Schoeffl GI, Higgins G. Immunohistochemical study of intimal microvessels in coronary atherosclerosis. *Am J Pathol*. 1993;143:164–172.
72. Ware JA. Too many vessels? Not enough? The wrong kind?: the VEGF debate continues. *Nat Med*. 2001;7:403–404.
73. Yuan C, Kerwin WS, Ferguson MS, Polissar N, Zhang S, Cai J, Hatsukami TS. Contrast-enhanced high resolution MRI for atherosclerotic carotid artery tissue characterization. *J Magn Reson Imaging*. 2002;15:62–67.
74. Lin W, Abendschein DR, Haacke EM. Contrast-enhanced magnetic resonance angiography of carotid arterial wall in pigs. *J Magn Reson Imaging*. 1997;7:183–190.
75. Maki JH, Wilson GJ, Lauffer RB, Wiesskoff RM, Yuan C. Apparent vessel wall inflammation detected using MS-325, a blood pool contrast agent. *Proc Int Soc Mag Reson Med*. 2001;9:639. Abstract.
76. Weiss CR, Arai AE, Bui MN, Agyeman KO, Waclawiw MA, Balaban RS, Cannon RO III. Arterial wall MRI characteristics are associated with elevated serum markers of inflammation in humans. *J Magn Reson Imaging*. 2001;14:698–704.
77. Schmitz SA, Coupland SE, Gust R, Winterhalter S, Wagner S, Kresse M, Semmler W, Wolf KJ. Superparamagnetic iron oxide-enhanced MRI of atherosclerotic plaques in Watanabe heritable hyperlipidemic rabbits. *Invest Radiol*. 2000;35:460–471.
78. Ruehm SG, Corot C, Vogt P, Kolb S, Debatin JF. Magnetic resonance imaging of atherosclerotic plaque with ultrasmall superparamagnetic particles of iron oxide in hyperlipidemic rabbits. *Circulation*. 2001;103:415–422.
79. Schmitz SA, Taupitz M, Wagner S, Wolf KJ, Beyersdorff D, Hamm B. Magnetic resonance imaging of atherosclerotic plaques using superparamagnetic iron oxide particles. *J Magn Reson Imaging*. 2001;14:355–361.
80. Johnstone MT, Botnar RM, Perez AS, Stewart R, Quist WC, Hamilton JA, Manning WJ. In vivo magnetic resonance imaging of experimental thrombosis in a rabbit model. *Arterioscler Thromb Vasc Biol*. 2001;21:1556–1560.
81. Toussaint JF, Southern JF, Fuster V, Kantor HL. Water diffusion properties of human atherosclerosis and thrombosis measured by pulse field gradient nuclear magnetic resonance. *Arterioscler Thromb Vasc Biol*. 1997;17:542–546.
82. Bradley WG Jr. MR appearance of hemorrhage in the brain. *Radiology*. 1993;189:15–26.
83. Moody AR. Direct imaging of deep-vein thrombosis with magnetic resonance imaging. *Lancet*. 1997;350:1073.
84. Fraser DG, Moody AR, Morgan PS, Martel AL, Davidson I. Diagnosis of lower-limb deep venous thrombosis: a prospective blinded study of magnetic resonance direct thrombus imaging. *Ann Intern Med*. 2002;136:89–98.
85. Moody AR, Liddicoat A, Krarup K. Magnetic resonance pulmonary angiography and direct imaging of embolus for the detection of pulmonary emboli. *Invest Radiol*. 1997;32:431–440.
86. Mugler JP III, Brookeman JR. Three-dimensional magnetization-prepared rapid gradient-echo imaging (3D MP RAGE). *Magn Reson Med*. 1990;15:152–157.
87. Corti R, Osende JL, Fayad ZA, Fallon JT, Fuster V, Mizsei G, Dickstein E, Drayer B, Badimon JJ. In vivo non-invasive detection and age definition of arterial thrombus by MRI. *J Am Coll Cardiol*. 2002;39:1366–1373.
88. Yu X, Song SK, Chen J, Scott MJ, Fuhrhop RJ, Hall CS, Gaffney PJ, Wickline SA, Lanza GM. High-resolution MRI characterization of human thrombus using a novel fibrin-targeted paramagnetic nanoparticle contrast agent. *Magn Reson Med*. 2000;44:867–872.
89. Flacke S, Fischer S, Scott MJ, Fuhrhop RJ, Allen JS, McLean M, Winter P, Sicard GA, Gaffney PJ, Wickline SA, Lanza GM. Novel MRI contrast agent for molecular imaging of fibrin: implications for detecting vulnerable plaques. *Circulation*. 2001;104:1280–1285.
90. Lauffer RB, Graham PB, Lahti KM, Nair S, Caravan P, Kolodziej A. Direct clot detection with MRI using a novel fibrin-targeted gadolinium agent. *Circulation*. 2000;102(suppl II):II-375. Abstract.
91. Johansson LO, Bjornerud A, Ahlstrom HK, Ladd DL, Fujii DK. A targeted contrast agent for magnetic resonance imaging of thrombus: implications of spatial resolution. *J Magn Reson Imaging*. 2001;13:615–618.
92. Brown BG, Zhao XQ, Sacco DE, Albers JJ. Arteriographic view of treatment to achieve regression of coronary atherosclerosis and to prevent plaque disruption and clinical cardiovascular events. *Br Heart J*. 1993;69:S48–S53.
93. Brown BG, Hillger L, Zhao XQ, Poulin D, Albers JJ. Types of change in coronary stenosis severity and their relative importance in overall progression and regression of coronary disease: observations from the FATS Trial: Familial Atherosclerosis Treatment Study. *Ann NY Acad Sci*. 1995;748:407–417.
94. McConnell MV, Aikawa M, Maier SE, Ganz P, Libby P, Lee RT. MRI of rabbit atherosclerosis in response to dietary cholesterol lowering. *Arterioscler Thromb Vasc Biol*. 1999;19:1956–1959.
95. Helft G, Worthley SG, Fuster V, Fayad ZA, Zaman AG, Corti R, Fallon JT, Badimon JJ. Progression and regression of atherosclerotic lesions: monitoring with serial noninvasive magnetic resonance imaging. *Circulation*. 2002;105:993–998.
96. Zhao XQ, Yuan C, Hatsukami TS, Frechette EH, Kang XJ, Maravilla KR, Brown BG. Effects of prolonged intensive lipid-lowering therapy on the characteristics of carotid atherosclerotic plaques in vivo by MRI: a case-control study. *Arterioscler Thromb Vasc Biol*. 2001;21:1623–1629.
97. Kang X, Polissar NL, Han C, Lin E, Yuan C. Analysis of the measurement precision of arterial lumen and wall areas using high-resolution MRI. *Magn Reson Med*. 2000;44:968–972.
98. Chan SK, Jaffer FA, Botnar RM, Kissinger KV, Goepfert L, Chuang ML, O'Donnell CJ, Levy D, Manning WJ. Scan reproducibility of magnetic resonance imaging assessment of aortic atherosclerosis burden. *J Cardiovasc Magn Reson*. 2001;3:331–338.
99. Yuan C, Lin E, Millard J, Hwang JN. Closed contour edge detection of blood vessel lumen and outer wall boundaries in black-blood MR images. *Magn Reson Imaging*. 1999;17:257–266.
100. Ladak HM, Thomas JB, Mitchell JR, Rutt BK, Steinman DA. A semi-automatic technique for measurement of arterial wall from black blood MRI. *Med Phys*. 2001;28:1098–1107.
101. Steinman DA, Thomas JB, Ladak HM, Milner JS, Rutt BK, Spence JD. Reconstruction of carotid bifurcation hemodynamics and wall thickness using computational fluid dynamics and MRI. *Magn Reson Med*. 2002;47:149–159.
102. Ladd ME, Quick HH, Debatin JF. Interventional MRA and intravascular imaging. *J Magn Reson Imaging*. 2000;12:534–546.
103. Yang X, Atalar E. Intravascular MR imaging-guided balloon angioplasty with an MR imaging guide wire: feasibility study in rabbits. *Radiology*. 2000;217:501–506.
104. Dion YM, Ben El Kadi H, Boudoux C, Gourdon J, Chakfe N, Traore A, Moisan C. Endovascular procedures under near-real-time magnetic resonance imaging guidance: an experimental feasibility study. *J Vasc Surg*. 2000;32:1006–1014.
105. Lardo AC, Yang X, Fayad ZA, Evers R, Chronos N. High resolution intravascular imaging following magnetic resonance guided aortic stent placement. *Circulation*. 2001;104(suppl II):II-764. Abstract.
106. Spuentrup E, Ruebben A, Schaeffter T, Manning WJ, Gunther RW, Buecker A. Magnetic resonance-guided coronary artery stent placement in a swine model. *Circulation*. 2002;105:874–879.
107. Yang X, Atalar E, Li D, Serfaty JM, Wang D, Kumar A, Cheng L. Magnetic resonance imaging permits in vivo monitoring of catheter-based vascular gene therapy. *Circulation*. 2001;104:1588–1590.
108. Schwartz RB, Hsu L, Wong TZ, Kacher DF, Zamani AA, Black PM, Alexander E III, Stieg PE, Moriarty TM, Martin CA, Kikinis R, Jolesz FA. Intraoperative MR imaging guidance for intracranial neurosurgery: experience with the first 200 cases. *Radiology*. 1999;211:477–488.
109. Smits HF, Bos C, van der Weide R, Bakker CJ. Endovascular interventional MR: balloon angioplasty in a hemodialysis access flow phantom. *J Vasc Interv Radiol*. 1998;9:840–845.

110. Breslow JL. Mouse models of atherosclerosis. *Science*. 1996;272:685–688.
111. Plump A. Atherosclerosis and the mouse: a decade of experience. *Ann Med*. 1997;29:193–198.
112. Smith JD, Breslow JL. The emergence of mouse models of atherosclerosis and their relevance to clinical research. *J Intern Med*. 1997;242:99–109.
113. Fuster V, Poon M, Willerson JT. Learning from the transgenic mouse: endothelium, adhesive molecules, and neointimal formation. *Circulation*. 1998;97:16–18.
114. Plump AS, Smith JD, Hayek T, Aalto-Setälä K, Walsh A, Verstuyf JG, Rubin EM, Breslow JL. Severe hypercholesterolemia and atherosclerosis in apolipoprotein E-deficient mice created by homologous recombination in ES cells. *Cell*. 1992;71:343–353.
115. Zhang SH, Reddick RL, Piedrahita JA, Maeda N. Spontaneous hypercholesterolemia and arterial lesions in mice lacking apolipoprotein E. *Science*. 1992;258:468–471.
116. Rubin EM, Krauss RM, Spangler EA, Verstuyf JG, Clift SM. Inhibition of early atherogenesis in transgenic mice by human apolipoprotein AI. *Nature*. 1991;353:265–267.
117. Boring L, Gosling J, Cleary M, Charo IF. Decreased lesion formation in CCR2<sup>-/-</sup> mice reveals a role for chemokines in the initiation of atherosclerosis. *Nature*. 1998;394:894–897.
118. Dansky HM, Charlton SA, Barlow CB, Tamminen M, Smith JD, Frank JS, Breslow JL. Apo A-I inhibits foam cell formation in apo E-deficient mice after monocyte adherence to endothelium. *J Clin Invest*. 1999;104:31–39.
119. Huber SA, Sakkinen P, Conze D, Hardin N, Tracy R. Interleukin-6 exacerbates early atherosclerosis in mice. *Arterioscler Thromb Vasc Biol*. 1999;19:2364–2367.
120. Tangirala RK, Tsukamoto K, Chun SH, Usher D, Pure E, Rader DJ. Regression of atherosclerosis induced by liver-directed gene transfer of apolipoprotein A-I in mice. *Circulation*. 1999;100:1816–1822.
121. Tsukamoto K, Tangirala R, Chun SH, Pure E, Rader DJ. Rapid regression of atherosclerosis induced by liver-directed gene transfer of apoE in apoE-deficient mice. *Arterioscler Thromb Vasc Biol*. 1999;19:2162–2170.
122. Desrumont C, Caillaud JM, Emmanuel F, Benoit P, Fruchart JC, Castro G, Branellec D, Heard JM, Duverger N. Complete atherosclerosis regression after human apoE gene transfer in apoE-deficient/nude mice. *Arterioscler Thromb Vasc Biol*. 2000;20:435–442.
123. Shah PK, Yano J, Reyes O, Chyu KY, Kaul S, Bisgaier CL, Drake S, Cercek B. High-dose recombinant apolipoprotein a-i(milano) mobilizes tissue cholesterol and rapidly reduces plaque lipid and macrophage content in apolipoprotein e-deficient mice: potential implications for acute plaque stabilization. *Circulation*. 2001;103:3047–3050.
124. Stein Y, Stein O. Does therapeutic intervention achieve slowing of progression or bona fide regression of atherosclerotic lesions? *Arterioscler Thromb Vasc Biol*. 2001;21:183–188.
125. Choudhury RP, Aguinaldo JG, Rong JX, Fallon JT, Fuster V, Fisher EA, Fayad ZA. Serial non-invasive high-resolution magnetic resonance imaging measures the progression of atherosclerosis in apolipoprotein E-deficient mice. *J Am Coll Cardiol*. 2001;37:1A–648A.
126. Choudhury RP, Aguinaldo JG, Rong JX, Kulak JL, Kulak AR, Reis ED, Fallon JT, Fuster V, Fisher EA, Fayad ZA. Atherosclerotic lesions in genetically modified mice quantified in vivo by non-invasive high-resolution magnetic resonance microscopy. *Atherosclerosis*. 2002;162:315–321.
127. Manka DR, Gilson W, Sarembock I, Ley K, Berr SS. Noninvasive in vivo magnetic resonance imaging of injury-induced neointima formation in the carotid artery of the apolipoprotein-E null mouse. *J Magn Reson Imaging*. 2000;12:790–794.
128. Fichtner KP, Schirmacher V, Griesbach A, Hull WE. In vivo 1H-NMR microimaging with respiratory triggering for monitoring adoptive immunotherapy of metastatic mouse lymphoma. *Magn Reson Med*. 1997;38:440–455.
129. Wiesmann F, Ruff J, Engelhardt S, Hein L, Dienesch C, Leupold A, Illinger R, Frydrychowicz A, Hiller KH, Rommel E, Haase A, Lohse MJ, Neubauer S. Dobutamine-stress magnetic resonance microimaging in mice: acute changes of cardiac geometry and function in normal and failing murine hearts. *Circ Res*. 2001;88:563–569.
130. Paigen B, Morrow A, Holmes PA, Mitchell D, Williams RA. Quantitative assessment of atherosclerotic lesions in mice. *Atherosclerosis*. 1987;68:231–240.
131. Weissleder R, Mahmood U. Molecular imaging. *Radiology*. 2001;219:316–333.
132. Weissleder R, Moore A, Mahmood U, Bhorade R, Benveniste H, Chioocca EA, Basilion JP. In vivo magnetic resonance imaging of transgene expression. *Nat Med*. 2000;6:351–355.
133. Louie AY, Huber MM, Ahrens ET, Rothbacher U, Moats R, Jacobs RE, Fraser SE, Meade TJ. In vivo visualization of gene expression using magnetic resonance imaging. *Nat Biotechnol*. 2000;18:321–325.
134. Davies MJ, Gordon JL, Gearing AJ, Pigott R, Woolf N, Katz D, Kyriakopoulos A. The expression of the adhesion molecules ICAM-1, VCAM-1, PECAM, and E-selectin in human atherosclerosis. *J Pathol*. 1993;171:223–229.
135. Wood KM, Cadogan MD, Ramshaw AL, Parums DV. The distribution of adhesion molecules in human atherosclerosis. *Histopathology*. 1993;22:437–444.
136. Nakashima Y, Raines EW, Plump AS, Breslow JL, Ross R. Upregulation of VCAM-1 and ICAM-1 at atherosclerosis-prone sites on the endothelium in the apoE-deficient mouse. *Arterioscler Thromb Vasc Biol*. 1998;18:842–851.
137. Sipkins DA, Gijbels K, Tropper FD, Bednarski M, Li KC, Steinman L. ICAM-1 expression in autoimmune encephalitis visualized using magnetic resonance imaging. *J Neuroimmunol*. 2000;104:1–9.
138. Sipkins DA, Cheresh DA, Kazemi MR, Nevin LM, Bednarski MD, Li KC. Detection of tumor angiogenesis in vivo by alphaVbeta3-targeted magnetic resonance imaging. *Nat Med*. 1998;4:623–626.
139. Anderson SA, Rader RK, Westlin WF, Null C, Jackson D, Lanza GM, Wickline SA, Kotyk JJ. Magnetic resonance contrast enhancement of neovasculature with alpha(v)beta(3)-targeted nanoparticles. *Magn Reson Med*. 2000;44:433–439.
140. Nunn AD, Linder KE, Tweedle MF. Can receptors be imaged with MRI agents? *Q J Nucl Med*. 1997;41:155–162.